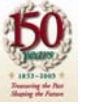


Effects of Scatterer Populations on Temperature Dependence of Backscattered Ultrasonic Energy

Jason W. Trabaugh,
R. Martin Arthur,
William L. Straube,
Eduardo G. Moros



Abstract

Theoretical and experimental evidence continues to suggest that backscattered ultrasonic energy changes predictably with temperature. Previously, theoretical results for a single scatterer showed that backscattered energy increases or decreases monotonically, depending on the lipid or aqueous nature of the scatterer. Recent experimental results showed that the same trend holds for measurements over an image region subtending multiple scatterers. To extend our theory to a more realistic tissue composition, we have developed methods for simulating ultrasonic images of multiple randomly distributed scatterers. In the simulations, the imaging system was described by its point-spread function, and the tissue medium was represented by discrete aqueous and lipid scatterers. Images were simulated to represent temperatures from 37 to 50°C by changing the scatterer amplitudes according to curves predicted previously for single scatterers. Change in backscattered energy (CBE) was computed for each image pixel, referenced to the initial image. To characterize CBE for a region, the means of the positive- and negative-changing pixels and the standard deviation of all pixels were computed. The region CBE showed the same monotonic increase and decrease as in experimental results and covered ranges similar to both prediction and experiment. Subsequent simulations included additive noise and showed striking agreement with experimental CBE measurements, replicating both an initial jump and noise throughout the range. These results support the use of CBE for noninvasive temperature estimation, showing that our model for the temperature dependence of CBE can be successfully applied to measurements from multiple scatterers. These simulation methods also provide a means for exploring limits on temperature accuracy and spatial resolution with varying imaging systems and tissue types.

Objectives

- Extend our theoretical model for change in backscattered energy from single scatterers to a medium containing multiple scatterers of multiple types
- Develop a simulation tool for guiding application of CBE to temperature estimation, for confirming past and present CBE results, for basic insight into observed phenomena, and for investigating spatial resolution and temperature accuracy.

Previous Results

- Original prediction showed temperature dependence of backscatter coefficient based on lipid or aqueous nature of a single, isolated scatterer
- Previous analysis showed measurable monotonic change in signal strength consistent across multiple tissue types both for 1D signals with individual segmented echoes and for 2D images analyzed for regions with multiple scatterers

Predicted Temperature Dependence of CBE

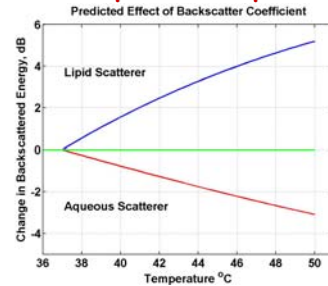


Figure 1. Predicted change in backscattered energy (CBE) with variation in temperature and associated changes in speed of sound for lipid and aqueous scatterer types.

Measured Temperature Dependence of CBE

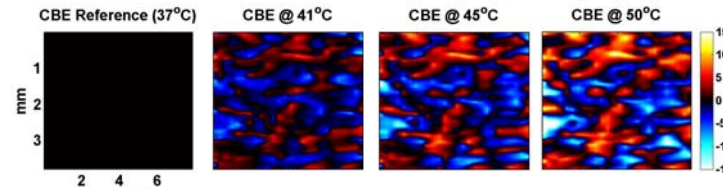


Figure 2. Measured change in CBE for a 3.5mm x 8mm region of bovine liver. The colormap shows positive and negative change as red and blue, respectively, to a maximum of 15 dB. The CBE at individual pixels appears to increase or decrease monotonically with temperature. Figure 3 shows the results of analyzing CBE images such as these, in their entirety, for multiple regions in multiple tissue types. Figure 5 below shows CBE images generated from ultrasound images simulated to represent hypothesized temperature-dependent changes in scatterer properties.

Analysis - Measured CBE

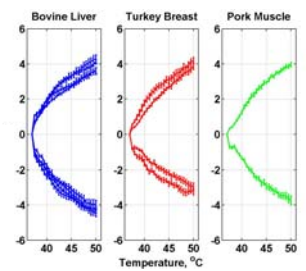


Figure 3. Measured positive and negative CBE for multiple regions in bovine liver, turkey breast and pork muscle showed consistent monotonic changes. Figures below show similar changes for images generated from hypothesized temperature dependence of individual scatterer properties.

Methods

Our simulations assume a linear systems model of image formation. The imaging system is described by its point-spread function. For the simulated images in Figure 4, the point-spread function was characterized by a 6MHz center frequency and lateral resolution of approximately 0.5 mm. Scatterers were represented as point sources with amplitudes obeying the temperature dependence as predicted in Figure 1. Initial amplitudes for each scatterer were generated from a uniform distribution. Initial positions were generated from a 2D uniform distribution over the region shown. For the simulated images of Figure 4, a total of 1000 lipid and 500 aqueous scatterers covered the 1cm x 1cm image region. Gaussian noise was added to the RF image for some experiments. The envelope of the RF image was generated using the Hilbert transform for display and analysis.

CBE measures were computed with reference to the initial image at 37°C. Analysis over the entire image region included a 3x3 moving average filter to reduce spurious contributions to the CBE.

Simulated Images - Original and CBE

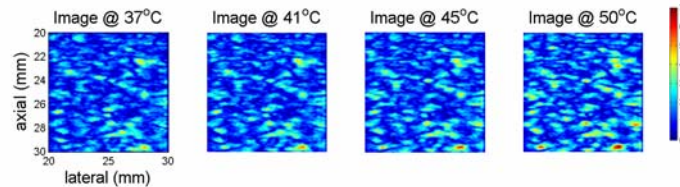


Figure 4. Simulated images representing tissue at 37, 41, 45 and 50°C. The tissue sample in these images was represented with 1000 lipid and 500 aqueous scatterers. Temperature-dependent change in the backscatter coefficient for each scatterer was based on published measurements of the speed of sound in fat and water. Relative changes in the energy, barely perceptible in these images, is quite clear in images of the CBE shown in Figure 2.

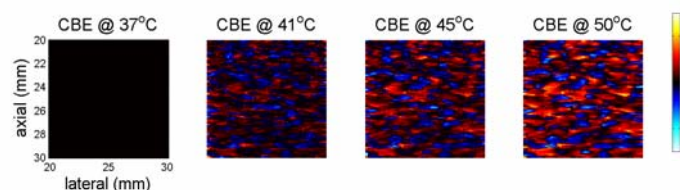


Figure 5. Images of the CBE for simulated images at 37, 41, 45 and 50°C, corresponding to the images in Figure 1. Positive and negative changes are shown in red and blue, respectively. Although the positive and negative changes are distributed evenly, the composite measures of change over this 1 cm² region are monotonic, as shown in Figures 3 through 7.

Analysis - CBE from Simulated Images

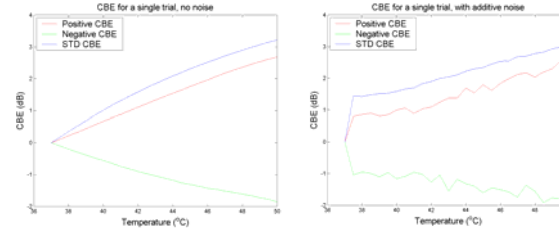


Figure 6. CBE curves generated from an image region as shown in Figure 5. Mean positive and negative CBE curves are shown, along with overall standard deviation. The plots on the left and right show the temperature dependence for images with and without additive noise, respectively.

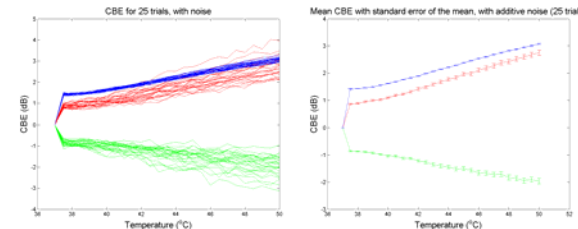


Figure 7. CBE curves from multiple trials with additive Gaussian noise. The plots on the left show results from individual trials. The plots on the right show the average over all trials.

Discussion

Analysis of CBE from measured 2D images shows monotonic changes in the CBE with temperature similar to that predicted for a single scatterer. The results shown here for images simulated from multiple scatterers are strikingly consistent with measured results:

- > CBE images generated from the simulations are similar to those generated from experimental images in both the distribution and amplitude of positive and negative changes
- > Analysis of the mean positive and negative changes, as well as overall standard deviation, also agree well with experimental results
- > Agreement between simulation and experiment results is especially high when additive signal noise is included in the image simulation, matching both noise in the CBE curve and an initial jump in the CBE.

Conclusions

These results provide further strong support to the investigation of CBE as a means for temperature estimation:

- > Images of multiple scatterers produce CBE in a similar manner to single, isolated scatterers
- > Our image simulation model provides a unique, effective means to explore variations in assumptions underlying our theoretical model, effects of varying scatterer populations, and limits on methods for estimating temperature from CBE, including spatial resolution and temperature accuracy.

Acknowledgement

This work was supported in part by NIH grant R21-CA90531 from the National Cancer Institute and the Wilkinson Trust at Washington University in St. Louis.